How to cite: Angew. Chem. Int. Ed. 2024, e202406931
doi.org/10.1002/anie.202406931

Non-equilibrium Systems

Photoinitiated Transient Self-Assembly in a Catalytically Driven Chemical Reaction Cycle

Jorge S. Valera, Álvaro López-Acosta, and Thomas M. Hermans**

Abstract: Chemically fueled chemical reaction networks (CRNs) are essential in controlling dissipative self-assembly. A key challenge in the field is to store chemical fuel-precursors or "pre-fuels" in the system that are converted into activating or deactivating fuels in a catalytically controlled CRN. In addition, real-time control over catalysis in a CRN by light is highly desirable, but so far not yet achieved. Here we show a catalytically driven CRN that is photoinitiated with 450 nm light, producing activated monomers that go on to perform transient self-assembly. Monomer activation proceeds via photoredox catalysis, converting the monomer alcohol groups into the corresponding aldehydes that self-assemble into large supramolecular fibers. Monomer deactivation is achieved by organometallic catalysis that relies on pre-fuel hydrolysis to release formate (i.e. the deactivating fuel). Additionally, irradiation with 305 nm light accelerates the release of formate by photo-uncaging the pre-fuel, leading to a factor of ca. 2 faster deactivation of the monomer. Overall, we show transient self-assembly upon visible light photoactivation, and tunable life-times by ultraviolet light.

Living cells rely on enzymatic chemical reaction networks (CRNs) to regulate the self-assembly process of supramolecular structures like actin filaments and microtubules.[1–5] The latter are responsible for biological processes like the formation of the mitotic spindle,[6,7] whereas the former play a key role in cell motility.[8–10] Inspired by nature, an increasing number of artificial CRNs have been used to control self-assembly events in the last decade.[11–13] Many of those CRNs[14,15] involve the consumption of a reagent or substrate (termed 'activating fuel') to activate a monomer prone to self-assemble. Subsequently, the monomer is deactivated by solvent hydrolysis,[16,17] due to same type of chemistry as used in activation (like thiol-ester[18] or thiol-disulfide[19] exchange), or by other means like redox chemistry or Michael additions.[20–22] So far, catalysis in artificial CRNs to control self-assembly has been achieved by enzymes,[23–25] transition metal catalysis[26,27] and organocatalysis,[28,29] and its benefits have been discussed recently.[30] Especially appealing is the ability to turn on the catalyst on demand or to modulate the catalysts activity in situ, permitting the storage of (excess) fuels in the system until a signal or a stimulus is provided,[31] altering at will the product steady state. Light is a perfect tool to this end, and to date has been used directly over the self-assembling moiety in the form of photoisomerization,[32–34] photoreduction,[35] photo-switchable molecular motors,[36] and with photocaged fuels in an enzymatic reaction network.[37] Compared to these systems, it can be envisioned that by modulating artificial catalytic systems with light, a higher degree of control over the transient species can be attained as well as the emergence of adaptive behavior due to feedback mechanisms between the different catalytic cycles.[12,30] Here we show a CRN that uses photoredox catalysis under visible light to convert deactivated monomer SachOL—to form (activated monomer) SachCHO that assembles into supramolecular fibers—and transition metal catalysis to deactivate SachCHO back to SachOL (Figure 1a). The slow hydrolysis of a pre-fuel releases formate as deactivation fuel, permitting to achieve a photoactivated and autonomous CRN. Since the pre-fuel also contains a photo-cleavable protecting group, the release of formate can be accelerated by ultraviolet light, leading to partial orthogonal light control with two different wavelengths.

We have previously reported chemically fueled gel-sol-gel[38,39] and sol-gel-sol-gel-sol transitions[40] using saccharide-based benzaldehyde derivative SachCHO. In the latter examples we converted the aldehyde of SachCHO to the hydroxy-sulfonate[38,39] or thiazinane[40] analogs that are negatively charged and therefore disassembled in aqueous solution. In the current work, we convert SachCHO to alcohol analog SachOL (see Section 2 in Supporting Information for synthetic details and characterization) which forms needle-like fibers in water (see Figure S1). However, fiber formation of SachOL is precluded in THF/0.5 M phosphate buffer mixtures (1/9 ratio, pH = 6) at the concentrations used in the remainder of the paper whereas SachCHO maintains its ability to form thin, long fibers sprouting from aster-like structures at 7–8 mM (see Figure S2).

[*] J. S. Valera, Á. López-Acosta, T. M. Hermans
IMDEA Nanociencia, C/ Faraday 9, 28049 Madrid, Spain
E-mail: jorge.santos@imdea.org
thomas.hermans@imdea.org
J. S. Valera, T. M. Hermans
Université de Strasbourg, CNRS, UMR7140, 4 Rue Blaise Pascal, 67081 Strasbourg, France

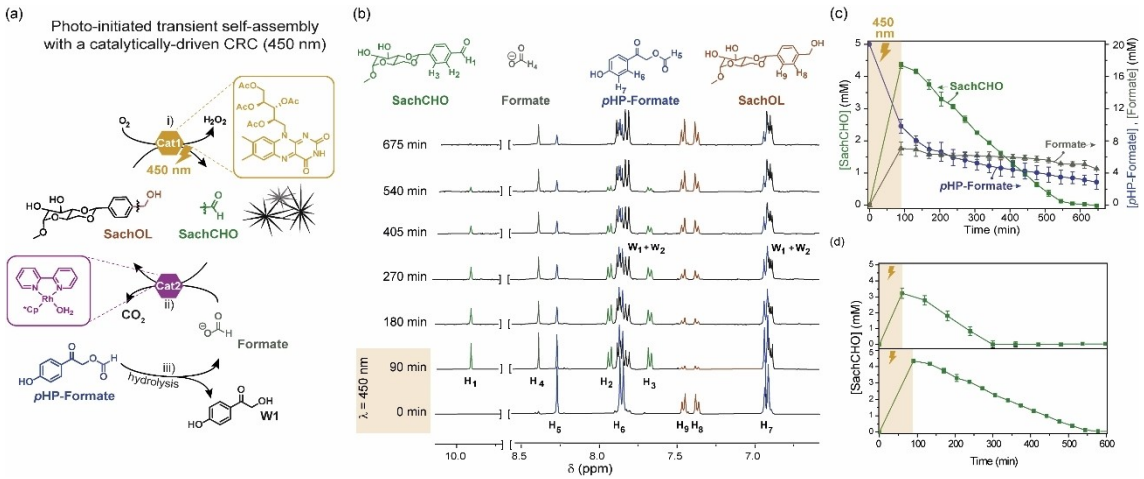

Figure 1. (a) Photoinitiated transient self-assembly of SachCHO fibers in a catalytically driven CRN. Oxidation of SachOL to SachCHO is achieved by using riboflavin tetraacetate (RFTA, **Cat1**) with 450 nm irradiation. Reduction of SachCHO to SachOL is attained by $[Cp^*Rh(Bpy)(H)]^+$, which is generated from $[Cp^*Rh(Bpy)(H_2O)]^{2+}$ (**Cat2**) using formate as a hydride source. Hydrolysis of *p*-hydroxyphenacyl formate (*p*HP-Formate) releases formate in the dark at longer times, producing the α-hydroxyketone (**W1**) as by-product. Steps i-iii are described in the main text. (b) ^{1}H NMR spectra (400 MHz, 298 K) of the CRN at different times. $[SachOL]_0 = 5$ mM, $[RFTA]_0 = 1$ mM, $[[Cp^*Rh(Bpy)(H_2O)]^{2+}]_0 = 1$ mM, $[p$HP-Formate$]_0 = 20$ mM in THF-d_8/0.5 M phosphate buffer pH = 6 1/9 mixtures. (c) Variation in the relative species concentration of SachCHO, Formate and *p*HP-Formate during the CRN obtained from Figure 1b. (d) Effect of the time of the 450 nm irradiation in SachCHO conversion in the CRN. Upper panel denotes 60 min of irradiation at 450 nm and lower panel 90 min of irradiation at 450 nm. The yellow/orange shaded regions and orange lightning bolt denote irradiation at 450 nm. Error bars are standard deviations over duplicate experiments.

The selective oxidation of benzylic alcohol SachOL to aldehyde SachCHO is achieved by riboflavin tetraacetate (RFTA, **Cat1** in Figure 1a) as photocatalyst upon 450 nm irradiation,[41–43] in high yields after 90 mins as shown by ^{1}H NMR experiments (Figure S3). RFTA is reduced while oxidizing the benzyl alcohol and is then regenerated by oxygen (i.e. the activating fuel), producing H_2O_2 as waste (step *i* in Figure 1a). This reaction is first order in SachOL (Figure S4–S5) showing an estimated halftime $t_{1/2} = 68$ min with 20 % **Cat1** loads (Table S1). The (deactivating) reduction of SachCHO to SachOL is quantitative through catalytic hydride transfer by $[Cp^*Rh(Bpy)(H)]^+$, which is generated in situ from the pre-catalyst $[Cp^*Rh(Bpy)(H_2O)]^{2+}$ (**Cat2** in Figure 1a, step *ii*) and formate as hydride source to produce CO_2 as waste (Figure S6). This reaction is zeroth order in SachCHO and first order in formate in the current conditions, indicating a more complex behavior in the case of **Cat2** which is out of the scope of this paper (see the section 'Kinetic Analysis Discussion' in Supporting Information and Figure S7–S8 and Tables S2–S3 for the estimated $t_{1/2}$ of SachCHO at different conditions).[44] To obtain a CRN capable of autonomous transient self-assembly upon photoactivation, we included *p*-hydroxyphenacyl formate (*p*HP-Formate in Figure 1) in the system, whose slow hydrolysis releases formate (step *iii* in Figure 1a) following pseudo-first order kinetics (Figure S9–S10, with $k_{exp} = 1.65 \pm 0.03 \times 10^{-3}$ min^{-1} and $t_{1/2} = 420$ min) and producing the α-hydroxyketone as by-product (**W1** in Figure 1a).[45] The release of formate from *p*HP-Formate permits to attain the conversion of SachCHO to SachOL after 600 min and paves the way to the study the complete cycle (Figure S11).

Combining **Cat1**, **Cat2**, and *p*HP-Formate into the full CRN, we can transiently and autonomously form SachCHO by irradiation with 450 nm as can be seen by ^{1}H NMR (Figure 1b, 1c and Figure S12). This approach enables us to control the amount of transient self-assembler formed by controlling the time of irradiation, obtaining ~60 % and ~85 % peak activation of SachOL to SachCHO after 60 min and 90 mins of irradiation, respectively (Figure 1d). The slow release of formate from the *p*HP-Formate, leads to the autonomous deactivation of SachCHO to SachOL with time.

Nevertheless, we observed that the stability of *p*HP-Formate in the cycle was lowered due to interactions with other components, a typical limitation in the development of CRNs.[46] Specifically, we noticed an increase in formate release from *p*HP-Formate in the presence of all the components of the cycle (Figure S13–S14, $k_{exp} = 4.1 \pm 0.1 \times 10^{-3}$ min^{-1} and $t_{1/2} = 171$ min) and, to a greater extent upon 450 nm irradiation in these conditions (compare it to Figure 1b and Figure S12, with an estimated $t_{1/2} = 90$ min). This latter interaction also generates the *p*-hydroxyacetophenone (**W2**) under 450 nm irradiation (Figure 1c and Figure S15 for the complete NMR spectra). We hypothesize that this enhanced release arises from the interaction of RFTA and the RFTA semiquinone radicals with *p*HP-Formate, respectively, in a similar way that has been reported for other radical species.[47]

The photoinitiated CRN was followed by bright field microscopy (Figure 2 and Video 1). For these experiments we increased the concentration of SachOL from 5 mM to 10 mM and reduced $[Cp^*Rh(Bpy)(H_2O)]^{2+}$ load to 15 % to allow nucleation-elongation and to obtain sufficiently large SachCHO fibers for optical microscopy (note the critical gel concentration of SachCHO is 21 mM for heating/cooling,[39] but at lower concentrations fibers still form).

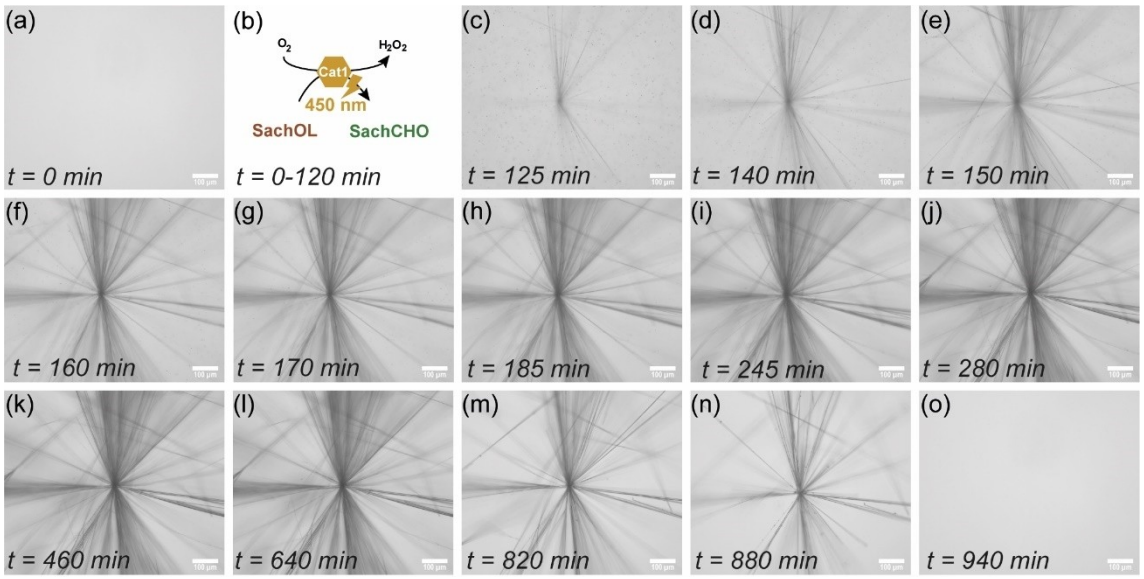

Figure 2. Bright field microscopy images of photoinitiated and catalytically driven-CRN at different stages: (a) A solution of SachOL, **Cat1**, **Cat2** and *p*HP-Formate, (b) irradiation with 450 nm activating light for 120 min to convert SachOL into SachCHO, (c–i) nucleation and elongation of SachCHO fibers into aster-like structures during the next 120 min, (j–l) SachCHO fibers remain stable during the following 500 min, (m–o) deactivation of SachCHO ensues followed by visible shrinking of its fibers at 800 min and complete disappearance due to its conversion into SachOL. $[SachOL]_0 = 10$ mM, **Cat1** $= [RFTA]_0 = 1.5$ mM, **Cat2** $= [[Cp^*Rh(Bpy)(H_2O)]^{2+}]_0 = 1.5$ mM, $[p$HP-Formate$]_0 = 30$ mM in THF-d_8/0.5 M phosphate buffer pH = 6 1/9 mixtures. All scale bars are 100 μm. See also Supporting Video 1.

A solution of SachOL, **Cat1**, **Cat2** and *p*HP-Formate is subjected to irradiation with λ = 450 nm during 120 mins to convert SachOL to SachCHO (Figure 2a–2b). At this time, nucleation and growth of asters-like structures characteristic of SachCHO takes place during the next ~125 min (Figure 2c–2i). After remaining ~500 min stable in solution (Figure 2j–2l), the continuous release of formate leads to deactivation and to the collapse of the SachCHO fibers with time (Figure 2m–2o).

An additional feature of using *p*HP-Formate as the pre-fuel, is that it can release formate much faster due to photo-uncaging upon irradiation with 305 nm light, a wavelength where it absorbs preferentially compared to RFTA (step *iv* in Figure 3a, and see Figure S16 for the absorption

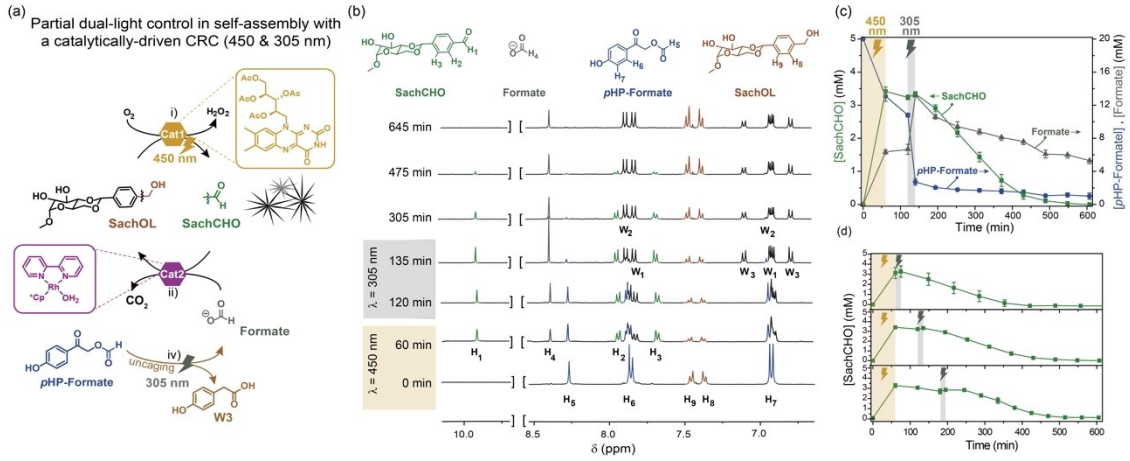

Figure 3. (a) Partial dual-light control over a catalytically driven CRN, forming transient SachCHO fibers. Oxidation and reduction proceed as described in Figure 1, but photocleavage of *p*HP-Formate with 305 nm light speeds up the release of formate producing *p*-hydroxyphenylacetic acid (**W3**) as the main by-product. Steps i–ii and iv are described in the main text. (b) ^{1}H NMR spectra (400 MHz, 298 K) at different times. $[SachOL]_0 = 5$ mM, $[RFTA]_0 = 1$ mM, $[[Cp^*Rh(Bpy)(H_2O)]^{2+}]_0 = 1$ mM, $[p$HP-Formate$]_0 = 20$ mM in THF-d_8/0.5 M phosphate buffer pH = 6 1/9 mixtures. (c) Relative species concentration of SachCHO, Formate and *p*HP-Formate under the conditions shown in Figure 3b. (d) Modulation of the lifetime of SachCHO by spacing the time between irradiation at 450 nm during 60 min and delaying irradiation at 305 nm (applied during 15 min) for 0 h (upper panel), 1 h (middle panel) and 2 h (lower panel). The yellow/orange shaded regions and orange lightning bolt denote irradiation at 450 nm and the grey shaded regions and lightning bolt at 305 nm. Error bars are standard deviations over duplicate experiments.

spectrum).[45] The photo uncaging of formate happens in less than 15 minutes in the presence of all the components of the cycle (Figure S17), producing *p*-hydroxyphenylacetic acid side product (**W3** in Figure 3a).[45] We explored the feasibility of the deactivation upon photo-uncaging of formate, achieving full conversion to SachOL after 400 min (see 20 % **Cat2** in Figure S18 and Table S4). This provides an additional tool to control the life-time of transient SachCHO self-assembly (Figure 3b–3c, Figure S19 and Figure S20 for complete NMR spectra). Although after the activation irradiation during 60 min ~30 % of formate (1.3 eq. in the conditions utilized) is released, we can still store enough pre-fuel in our system to accelerate deactivation by a factor ~1.8 using 305 nm light (Figure S21–22, note that the remaining pre-fuel concentration without deactivating 305 nm light is at least 2x times higher than the one observed with irradiation, which explains this enhancement in agreement with Figure S8 and Table S3). As shown in Figure 3d, after 60 min irradiation with 450 nm, we can delay the triggering of the deactivation for 0 h (upper panel), 1 h (middle panel) and 2 h (lower panel), thus controlling the lifetime of SachCHO under the same conditions and concentrations of all components of the cycle (notice that the estimated SachCHO halftimes are $t_{1/2} = 250$ min, 315 min, and 360 min, respectively).

In Scheme S1 we showcase the complete CRN with the three coupled cycles, the interactions between all each of the components of the system and references to the specific supporting Figures that demonstrate the interactions.

We also followed the 450/305 nm CRN of Figure 3a by bright field microscopy (Figure S23–S24 and Video 2) in similar conditions than those of Figure 2. The formed aster-like structures are similar, and deactivation by 305 nm light leads to slightly faster disappearance (as compared to Figure 2), thus providing up to a factor ~1.8 control over the life-time of the transient structures.

Overall, we have shown that transient self-assembly can be photoinitiated by visible 450 nm light. Our catalytically driven CRN relies on a photoredox catalyst for activation/assembly and transition metal catalysis combined with a pre-fuel for deactivation/disassembly. The lifetime of the transient assemblies can be controlled by a second wavelength (305 nm) by less than a factor two. Our current approach constitutes a first step towards full photocatalytic control in fuel-driven self-assembly, offering more precise control over the lifetime of the transient species at the same catalyst loading, abundant storage of (pre-)fuels in the system until needed and to sustain long-lived non-equilibrium steady states. Future systems with more stable pre-fuels than *p*-hydroxyphenacyl formate (like those based on soluble novel coumarin derivatives in water and/or *meso*-Methyl BODIPY based photocages)[48–50] would be desirable to further extend the usable time-window of this catalytic CRN. We foresee spatiotemporal control over forming and destroying supramolecular fibers as a basis for μm-sized soft robots,[51,52] where abundant and stable pre-fuels would enable their prolonged operation and motility.

Acknowledgements

J.S.V. and T.M.H. acknowledge funding from ERC-2017-STG "Life-Cycle" (757910). A.L-A. acknowledges the European Union's Horizon 2020 Research and Innovation Program under the Marie Skłodowska-Curie grant agreement no. 812868 for Ph.D. funding. We thank Marten L. Ploeger and Alex Blokhuis for fruitful discussions.

Conflict of Interest

There are no conflicts to declare.

Data Availability Statement

The data that support the findings of this study are available from the corresponding author upon reasonable request.

Keywords: Dissipative self-assembly · out-of-equilibrium · chemical reaction cycles · photoredox catalysis · chemical fuels

[1] A. S. Y. Wong, W. T. S. Huck, *Beilstein J. Org. Chem.* **2017**, *13*, 1486–1497. https://doi.org/10.3762/bjoc.13.147.
[2] K. Rottner, J. Faix, S. Bogdan, S. Linder, E. Kerkhoff, *J. Cell Sci.* **2017**, *130*(20), 3427–3435. https://doi.org/10.1242/jcs.206433.
[3] E. M. Mandelkow, E. Mandelkow, R. A. Milligan, *J. Cell Biol.* **1991**, *114*(5), 977–991. https://doi.org/10.1083/jcb.114.5.977.
[4] C. Conde, A. Cáceres, *Nat. Rev. Neurosci.* **2009**, *10*(5), 319–332. https://doi.org/10.1038/nrn2631.
[5] D. A. Fletcher, R. D. Mullins, *Nature* **2010**, *463*(7280), 485–492. https://doi.org/10.1038/nature08908.
[6] P. Bastiaens, M. Caudron, P. Niethammer, E. Karsenti, *Trends Cell Biol.* **2006**, *16*(3), 125–134. https://doi.org/10.1016/j.tcb.2006.01.005.
[7] S. L. Prosser, L. Pelletier, *Nat. Rev. Mol. Cell Biol.* **2017**, *18*(3), 187–201. https://doi.org/10.1038/nrm.2016.162.
[8] T. J. Mitchison, L. P. Cramer, *Cell* **1996**, *84*(3), 371–379. https://doi.org/10.1016/S0092-8674(00)81281-7.
[9] T. D. Pollard, G. G. Borisy, *Cell* **2003**, *112*(4), 453–465. https://doi.org/10.1016/S0092-8674(03)00120-X.
[10] L. Blanchoin, R. Boujemaa-Paterski, C. Sykes, J. Plastino, *Physiol. Rev.* **2014**, *94*(1), 235–263. https://doi.org/10.1152/physrev.00018.2013.
[11] S. A. P. Van Rossum, M. Tena-Solsona, J. H. Van Esch, R. Eelkema, J. Boekhoven, *Chem. Soc. Rev.* **2017**, *46*(18), 5519–5535. https://doi.org/10.1039/c7cs00246 g.
[12] M. Weißenfels, J. Gemen, R. Klajn, *Chem* **2021**, *7*(1), 23–37. https://doi.org/10.1016/j.chempr.2020.11.025.
[13] A. Sharko, D. Livitz, S. De Piccoli, K. J. M. Bishop, T. M. Hermans, *Chem. Rev.* **2022**, *122*(13), 11759–11777. https://doi.org/10.1021/acs.chemrev.1c00958.
[14] N. Singh, G. J. M. Formon, S. De Piccoli, T. M. Hermans, *Adv. Mater.* **2020**, *32*(20), 1–6. https://doi.org/10.1002/adma.201906834.
[15] B. Rieß, R. K. Grötsch, J. Boekhoven, *Chem* **2020**, *6*(3), 552–578. https://doi.org/10.1016/j.chempr.2019.11.008.
[16] J. Boekhoven, A. M. Brizard, K. N. K. Kowlgi, G. J. M. Koper, R. Eelkema, J. H. Van Esch, *Angew. Chem. Int. Ed.* **2010**, *49*(28), 4825–4828. https://doi.org/10.1002/anie.201001511.

[17] M. Tena-Solsona, B. Rieß, R. K. Grötsch, F. C. Löhrer, C. Wanzke, B. Käsdorf, A. R. Bausch, P. Müller-Buschbaum, O. Lieleg, J. Boekhoven, *Nat. Commun.* **2017**, *8*, 15895. https://doi.org/10.1038/ncomms15895.
[18] A. K. Dambenieks, P. H. Q. Vu, T. M. Fyles, *Chem. Sci.* **2014**, *5*(9), 3396–3403. https://doi.org/10.1039/C4SC01258E.
[19] S. M. Morrow, I. Colomer, S. P. Fletcher, *Nat. Commun.* **2019**, *10*(1), 1011. https://doi.org/10.1038/s41467-019-08885-9.
[20] J. Leira-Iglesias, A. Tassoni, T. Adachi, M. Stich, T. M. Hermans, *Nat. Nanotechnol.* **2018**, *13*(11), 1021–1027. https://doi.org/10.1038/s41565-018-0270-4.
[21] B. Klemm, R. W. Lewis, I. Piergentili, R. Eelkema, *Nat. Commun.* **2022**, *13*(1), 6242. https://doi.org/10.1038/s41467-022-33810-y.
[22] A. Sharko, B. Spitzbarth, T. M. Hermans, R. Eelkema, *J. Am. Chem. Soc.* **2023**, *145*(17), 9672–9678. https://doi.org/10.1021/jacs.3c00985.
[23] S. Debnath, S. Roy, R. V. Ulijn, *J. Am. Chem. Soc.* **2013**, *135*(45), 16789–16792. https://doi.org/10.1021/ja4086353.
[24] S. Dhiman, A. Jain, M. Kumar, S. J. George, *J. Am. Chem. Soc.* **2017**, *139*(46), 16568–16575. https://doi.org/10.1021/jacs.7b07469.
[25] A. Sorrenti, J. Leira-Iglesias, A. Sato, T. M. Hermans, *Nat. Commun.* **2017**, *8*, 15899. https://doi.org/10.1038/ncomms15899.
[26] C. S. Wood, C. Browne, D. M. Wood, J. R. Nitschke, *ACS Cent. Sci.* **2015**, *1*(9), 504–509. https://doi.org/10.1021/acscentsci.5b00279.
[27] I. Colomer, S. M. Morrow, S. P. Fletcher, *Nat. Commun.* **2018**, *9*(1), 2239. https://doi.org/10.1038/s41467-018-04670-2.
[28] S. Bal, K. Das, S. Ahmed, D. Das, *Angew. Chem. Int. Ed.* **2019**, *58*(1), 244–247. https://doi.org/10.1002/anie.201811749.
[29] M. P. van der Helm, C.-L. Wang, B. Fan, M. Macchione, E. Mendes, R. Eelkema, *Angew. Chem. Int. Ed.* **2020**, *59*(46), 20604–20611. https://doi.org/10.1002/anie.202008921.
[30] M. P. van der Helm, T. de Beun, R. Eelkema, *Chem. Sci.* **2021**, *12*(12), 4484–4493. https://doi.org/10.1039/D0SC06406H.
[31] M. P. van der Helm, G. Li, M. Hartono, R. Eelkema, *J. Am. Chem. Soc.* **2022**, *144*(21), 9465–9471. https://doi.org/10.1021/jacs.2c02695.
[32] P. K. Kundu, D. Samanta, R. Leizrowice, B. Margulis, H. Zhao, M. Börner, T. Udayabhaskararao, D. Manna, R. Klajn, *Nat. Chem.* **2015**, *7*(8), 646–652. https://doi.org/10.1038/nchem.2303.
[33] R. Chen, S. Neri, L. J. Prins, *Nat. Nanotechnol.* **2020**, *15*(10), 868–874. https://doi.org/10.1038/s41565-020-0734-1.
[34] K. Nakamura, W. Tanaka, K. Sada, R. Kubota, T. Aoyama, K. Urayama, I. Hamachi, *J. Am. Chem. Soc.* **2021**, *143*(46), 19532–19541. https://doi.org/10.1021/jacs.1c09172.
[35] C. Chen, J. S. Valera, T. B. M. Adachi, T. M. Hermans, *Chem. - Eur. J.* **2023**, *29*(1), e202202849. https://doi.org/10.1002/chem.202202849.
[36] F. Xu, S. Crespi, G. Pacella, Y. Fu, M. C. A. Stuart, Q. Zhang, G. Portale, B. L. Feringa, *J. Am. Chem. Soc.* **2022**, *144*(13), 6019–6027. https://doi.org/10.1021/jacs.2c01063.
[37] J. Deng, D. Bezold, H. J. Jessen, A. Walther, *Angew. Chem.* **2020**, *132*(29), 12182–12190. https://doi.org/10.1002/ange.202003102.
[38] N. Singh, B. Lainer, G. J. M. Formon, S. De Piccoli, T. M. Hermans, *J. Am. Chem. Soc.* **2020**, *142*(9), 4083–4087. https://doi.org/10.1021/jacs.9b11503.
[39] N. Singh, A. Lopez-Acosta, G. J. M. Formon, T. M. Hermans, *J. Am. Chem. Soc.* **2022**, *144*(1), 410–415. https://doi.org/10.1021/jacs.1c10282.
[40] T. M. Hermans, N. Singh, *Angew. Chem. Int. Ed.* **2023**, *62*(23), e202301529. https://doi.org/10.1002/anie.202301529.
[41] R. Cibulka, R. Vasold, B. König, *Chem. - Eur. J.* **2004**, *10*(24), 6223–6231. https://doi.org/10.1002/chem.200400232.
[42] H. Schmaderer, P. Hilgers, R. Lechner, B. König, *Adv. Synth. Catal.* **2009**, *351*(1–2), 163–174. https://doi.org/10.1002/adsc.200800576.
[43] J. Daďová, S. Kümmel, C. Feldmeier, J. Cibulková, R. Pažout, J. Maixner, R. M. Gschwind, B. König, R. Cibulka, *Chem. - Eur. J.* **2013**, *19*(3), 1066–1075. https://doi.org/10.1002/chem.201202488.
[44] C. Leiva, H. C. Lo, R. H. Fish, *J. Organomet. Chem.* **2010**, *695*(2), 145–150.
[45] R. S. Givens, M. Rubina, J. Wirz, *Photochem. Photobiol. Sci.* **2012**, *11*(3), 472–488. https://doi.org/10.1039/C2PP05399 C.
[46] B. Fan, Y. Men, S. A. P. van Rossum, G. Li, R. Eelkema, *ChemSystemsChem* **2020**, *2*(1), e1900028. https://doi.org/10.1002/syst.201900028.
[47] E. Speckmeier, K. Zeitler, *ACS Catal.* **2017**, *7*(10), 6821–6826. https://doi.org/10.1021/acscatal.7b02117.
[48] M. Bojtár, A. Kormos, K. Kis-Petik, M. Kellermayer, P. Kele, *Org. Lett.* **2019**, *21*(23), 9410–9414. https://doi.org/10.1021/acs.orglett.9b03624.
[49] P. Shrestha, D. Kand, R. Weinstain, A. H. Winter, *J. Am. Chem. Soc.* **2023**, *145*(32), 17497–17514. https://doi.org/10.1021/jacs.3c01682.
[50] Y. Li, M. Wang, F. Wang, S. Lu, X. Chen, *Smart Molecules* **2023**, *1*(1), e20220003. https://doi.org/10.1002/smo.20220003.
[51] A. H. Gelebart, D. Jan Mulder, M. Varga, A. Konya, G. Vantomme, E. W. Meijer, R. L. B. Selinger, D. J. Broer, *Nature* **2017**, *546*(7660), 632–636. https://doi.org/10.1038/nature22987.
[52] C. Li, A. Iscen, H. Sai, K. Sato, N. A. Sather, S. M. Chin, Z. Álvarez, L. C. Palmer, G. C. Schatz, S. I. Stupp, *Nat. Mater.* **2020**, *19*(8), 900–909. https://doi.org/10.1038/s41563-020-0707-7.

Manuscript received: April 11, 2024
Accepted manuscript online: May 21, 2024
Version of record online: ■■, ■■

Communications

Non-equilibrium Systems

J. S. Valera,* Á. López-Acosta,
T. M. Hermans* —— **e202406931**

Photoinitiated Transient Self-Assembly in a Catalytically Driven Chemical Reaction Cycle

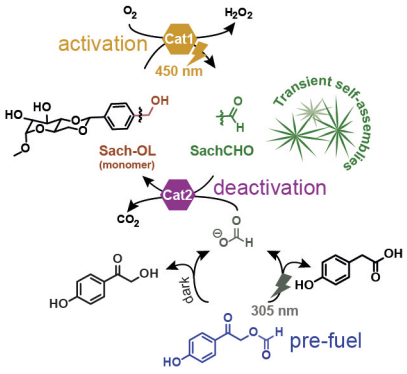

We show a catalytically-driven chemical reaction network (CRN) photoinitiated with 450 nm light. By combining photoredox and organometallic catalysis relying on pre-fuel hydrolysis to release deactivating fuel, we can control the formation of transient supramolecular fibers. Irradiation with 305 nm light accelerates the release of deactivating fuel, leading to faster deactivation of the monomer. Overall, we show transient self-assembly upon visible light activation, and tunable life-times by ultraviolet light.